

<sup>1</sup> This version of the article has been accepted for publication, after peer review (when applicable) and is subject to Springer Nature's AM terms of use (<https://www.springernature.com/gp/open-research/policies/accepted-manuscript-terms>), but is not the Version of Record and does not reflect post-acceptance improvements, or any corrections. The Version of Record is available online at: <http://dx.doi.org/10.1007/s11071-016-2883-1>.

# Dynamic probabilistic design approach of high-pressure turbine blade-tip radial running clearance

Cheng-Wei Fei · Yat-Sze Choy · Dian-Yin Hu ·  
Guang-Chen Bai · Wen-Zhong Tang

C.-W. Fei Y.-S. Choy  
Department of Mechanical Engineering, The Hong Kong  
Polytechnic University, Hung Hom, Kowloon, Hong Kong,  
People's Republic of Chinae-mail: feicw544@163.com

C.-W. Fei D.-Y. Hu G.-C. Bai  
School of Energy and Power Engineering,  
Beijing University of Aeronautics and Astronautics, Beijing 100191, People's Republic of China

W.-Z. Tang  
School of Computer Science and Engineering, Beijing University of Aeronautics and Astronautics,  
Beijing 100191, People's Republic of China

**Abstract** To develop the high performance and high reliability of turbomachinery just like an aeroengine, distributed collaborative time-varying least squares support vector machine (LSSVM) (called as DC- T-LSSVM) method was proposed for the dynamic probabilistic analysis of high-pressure turbine blade- tip radial running clearance (BTRRC). For structural transient probabilistic analysis, time-varying LSSVM (called as T-LSSVM) method was developed by improving LSSVM, and the mathematical model of the T-LSSVM was established. The mathematical model of DC-T-LSSVM was built based on T-LSSVM and distributed collaborative strategy. Through the dynamic probabilistic analysis of BTRRC with respect to the nonlinearity of material property and the dynamics of thermal load and centrifugal force load, the probabilistic distributions and features of different influential parameters on BTRRC, such as rotational speed, the temperature of gas, expansion coefficients, the surface coefficients of heat transfer and the deformations of disk, blade and casing, are obtained. The deformations of turbine disk, blade and casing, the rotational speed and the temperature of gas significantly influence BTRRC. Turbine disk and blade perform the positive effects on the BTRRC, while turbine casing has the negative impact. The comparison of four methods (Monte Carlo method, T-LSSVM, DCERSM and DC- T-LSSVM) reveals that the DC-T-LSSVM reshapes the possibility of the probabilistic analysis of complex turbomachinery and improves the computational efficiency while preserving the accuracy. The efforts offer a useful insight for rapidly designing and optimizing the BTRRC dynamically from a probabilistic perspective.

**Keywords** Blade-tip radial running clearance Dynamic probabilistic analysis Distributed collaborative strategy Time-varying LSSVM Multi-object multi-disciplinary

## 1. Introduction

The blade-tip radial clearance of high-pressure turbine is defined as the radial distance between the end of a turbine blade-tip and the casings, which seriously influences the reliability and performance of gas turbines (aeroengine) such as working efficiency, specific fuel consumption, engine thrust and flight time of aircraft [1]. The blade-tip radial running clearance (BTRRC) of high-pressure turbine is a

transient (dynamic) blade-tip radial clearance during the period of aeroengine operation [2], which is considered as a very crucial component in the design of gas turbines. Increasing demands for the higher working efficiency and higher operating temperatures require more stringent tolerances on BTRRC [3]. In this regard, a strategic control of a reasonable blade-tip clearance is required such that the working efficiency can be increased, the performance can be improved, services life can be expanded, and the specific fuel consumption can be effectively reduced. Therefore, the determination and design of an approach for controlling BTRRC is one of the key techniques for developing the high reliability and high performance of gas turbine, especially for an aeroengine.

Previous efforts have quantified the transient BTRRC using both experimental and numerical results [6–11]. For instance, Jia et al. [6] studied the effect of rotor vibration on tip clearance variation and fast active control; Annette et al. [7] investigated the thermal effects on gas turbine tip clearance in the transients region by finite element model and experiment; Forssell [8] analyzed the flight clearance using global nonlinear optimization-based search algorithms; Hennecke et al. [9] developed the turbine tip clearance control in gas turbine engines; Kypuros et al. [10] established a reduced model for prediction of thermal and rotational effects on turbine tip clearance; Pillidis et al. [11] built the prediction models of tip clearance changes in gas turbines. These researchers made many efforts on the analyses and experiments in order to identify the dynamic characteristics of mechanisms for the control of BTRRC due to the deflections of disk, blade and casing. Most of these works focus on the deterministic analysis, which assures the security of BTRRC by a reserved tip clearance allowance. Without considering the uncertainty of impact parameters in the deterministic analysis, the deterministic approach has some blindness. For example, too small reserved clearance leads to the rub between blade-tip and casing during aeroengine operation, and too large reserved clearance reduces the working efficiency of aeroengine. In other words, it is difficult to balance two aspects of the contradiction of no rubbing and clearance reduction [12]. In fact, many influencing parameters on BTRRC hold obviously randomness so that the BTRRC at a time point is random variable during aeroengine operation. To design and control the BTRRC in a more reasonable way, the variation of other physical parameters such as thermal and mechanical transient stresses should be considered at the same time, so that the change pattern of BTRRC can be described objectively and accurately during aeroengine operation from a probabilistic perspective.

The computational load of BTRRC probabilistic analysis is very large because of thousands of looping calculations with multi-object, multi-discipline, non-linearity and dynamics. Monte Carlo (MC) method, an effective technique for simple structural response for probabilistic analysis [12–14], is unsuitable due to unacceptable computational efficiency for the nonlinear dynamic, multi-object and multi-discipline (MOMD) of complex machinery. Many attempts to solve the effects of the uncertainties have led to the development of the other probabilistic analysis method—response surface method (RSM, also called surrogate model), and it was widely employed in many fields [15–20]. Currently, RSM is effective to continuously improve the accuracy and efficiency in structural reliability by reducing the number of expensive finite element analysis [21–25]. The typical surrogate models include polynomial response surface method [15,16,21,22] and support vector machine (SVM) [25–32]. The polynomial response surface method fits a low-order polynomial to a set of experimental data by least squares regression analysis [15,16,31,32]. The SVM which is regarded as an intelligent statistical learning method with implicit performance function has been applied to the reliability analysis and optimal design of complex structure instead of the polynomial response surface method, because SVM has the advantages of smaller training samples, higher computational accuracy and efficiency. Just because of these advantages, the SVM is also applied to anomaly detection for signals [30,31] and nonlinear predictive control of controller [32]. To further improve the computing speed for SVM model, the least squares SVM (LSSVM) was

developed and proved to be an effective method for structural steady reliability analysis [26]. However, for the time-varying characteristics of the nonlinear dynamic MOMD probabilistic analysis of complex structure, the LSSVM is unable to be directly adopted. It is because of two important issues: (1) LSSVM can only approximate the performance function at one particular time within time domain, resulting from it belongs to partial response surface method; (2) it is difficult to accomplish the probabilistic analysis of multiple models by the LSSVM.

To solve the first problem on the surrogate model, this paper proposes the time-varying least squares support vector machine method (T-LSSVM). This approach implements multiple calculations under different time points in a time domain where the responses of all calculations in the time domain is process response, and then selects the extremum (maximum or minimum value) of the process response during the time domain as the output response of LSSVM. The output response is the extremum response within the whole time domain, so the T-LSSVM is a global response surface method and outperforms the LSSVM in terms of high efficiency and high precision. In this regard, the mathematical model of T-LSSVM is to be established.

To tackle the second issue with the nonlinear dynamic MOMD feature, the distributed collaborative T-LSSVM, denoted by DC-T-LSSVM, is developed for the probabilistic analysis of complex machine by integrating the distributed collaborative strategy [2,33] and T-LSSVM.

In what follows, Sect. 2 outlines the issue formation of blade-tip radial clearance design. In Sect. 3, the distributed collaborative time-varying LSSVM for probabilistic analysis is to be studied, including the introduction of LSSVM, the establishment of mathematical model for T-LSSVM and DC-T-LSSVM. Section 4 discusses the basic thought of BTRRC probabilistic analysis. Section 5 focuses on the dynamic deterministic analyses of BTRRC. Section 6 studies the dynamic probabilistic analyses of three objects of BTRRC with T-LSSVM. The dynamic probabilistic analysis of blade-tip radial clearance with DC-T-LSSVM and the validation of DC-T-LSSVM are finished in Sect. 7. The main conclusions and the outlooks for future work are given in Sect. 8.

## 2. Issue formation of blade-tip radial clearance design

The BTRRC of high-pressure turbine would seriously influence the performance and reliability of aeroengine system. The sketch of BTRRC is shown in Fig. 1.

In line with engineering experiences, the reduction of BTRRC is beneficial to decrease specific fuel consumption, extend air flight time, expand compressor surge margin and increase payload [2,3]. For instance, when the ratio of blade-tip clearance to blade length decreases by 1 %, it is promising to improve by 0.8–1.2 % in the efficiency of compressor or turbine, to decline by 2 and 1.5 % in the specific fuel consumption of double-rotor turbofan engine and turboshaft engine, respectively [2]. In fact, BTRRC always varies with different operating conditions as illustrated in Fig. 2.

Figure 2 shows that aeroengine performance can be maximized at the cruise phase, whereas contact risk can be controlled at the takeoff–climb phase. If the reserved blade-tip clearance is too small, the friction fault and even the critical failures such as blade fracture and casing damage between blade-tip and casing may occur [5–9]. Therefore, the BTRRC of aeroengine has to be dynamically analyzed and even actively controlled in order to keep aeroengine with a reasonable clearance in various working conditions.

Most previous efforts in the BTRRC design of gas turbine are completed from a deterministic analysis perspective [3–11]. The deterministic method cannot quantitatively trade off the two aspects (the

reduction of blade-tip clearance and no friction) of the contradictory owing to no considering the randomness of various parameters influencing the clearance. In addition, the BTRRC design of high-pressure aeroengine turbine creates numerous dynamic assembly problems between rotor and stator that includes many objects such as disk, blade and casing. There are also many mechanical mechanisms such as heat transfer and rotor dynamics [2,3,5–11]. Undoubtedly, the BTRRC probabilistic analysis is also a typical MOMD nonlinear dynamic analysis issue from a probabilistic perspective [28]. To balance the reliability and efficiency of gas turbine, the BTRRC should be improved by probabilistic analysis, which is able to acquire the effect probabilities and distribution features of random parameters, and the distribution features and optimum design value of BTRRC. To improve the computational efficiency and accuracy of BTRRC probabilistic analysis, the DC-T-LSSVM is presented for nonlinear dynamic MOMD probabilistic analysis.

### 3. Distributed collaborative time-varying LSSVM for probabilistic analysis

In order to solve the nonlinear dynamic MOMD probabilistic analysis of complex machinery, the T-LSSVM and DC-T-LSSVM are proposed in this section.

#### 3.1 LSSVM

SVM is an important surrogate model based on intelligent statistical learning theory [26,27,34] and holds many advantages such as small samples to fit model, nonlinear mapping, good robustness, avoiding dimension disaster. LSSVM adopts the linear equation in low-dimensional space replacing the quadratic programming problem in high-dimensional space to improve computational efficiency and computing precision, by taking the term of squared error as the objective function and regarding an equation as the constraints [11,21]. The basic thought and mathematical model of LSSVM are summarized as follows.

From a certain kind of assumed distribution  $P(\mathbf{x}, y)$  ( $\mathbf{x} \in \mathbf{R}^n$  and  $y \in \mathbf{R}$ ) and the generated sampling points  $(\mathbf{x}_i, y_i)_{i=1,2,\dots,l}$ , a set of functions  $F$  which maps a point in the space  $\mathbf{R}^n$  onto the space  $\mathbf{R}$  is denoted by

$$F = \{f(\mathbf{x}, \boldsymbol{\omega}), \boldsymbol{\omega} \in \Lambda | f: \mathbf{R}^n \rightarrow \mathbf{R}\}, \quad (1)$$

in which  $\Lambda$  is a set of parameters and  $\boldsymbol{\omega}$  is an undetermined parameter vector.

The regression object is to find a function  $f \in F$  to make Eq. (1) have the lowest expected risk as

$$R(f) = \int l[y - f(\mathbf{x}, \boldsymbol{\omega})] dP(\mathbf{x}, y), \quad (2)$$

here  $l[y - f(\mathbf{x}, \boldsymbol{\omega})]$  is an error function [21] and defined as

$$l[y - f(\mathbf{x}, \boldsymbol{\omega})] = \max\{0, |y - f(\mathbf{x}, \boldsymbol{\omega})| - \varepsilon\}, \quad (3)$$

where  $\varepsilon > 0$ .

For the nonlinear regression, function  $f$  can be determined by the following method.

Each sampling point is mapped by a nonlinear function  $\phi$  onto the high-dimensional space to conduct the linear regression, and then, the original space nonlinear regression effect is attained. Thus, the function  $f$  is rewritten as

$$f(\mathbf{x}, \boldsymbol{\omega}) = \boldsymbol{\omega} \cdot \boldsymbol{\varphi}(\mathbf{x}) + b. \quad (4)$$

Obviously, the problem of solving the regression function is transformed into obtaining the following optimal solution

$$\min \frac{1}{2} \|\boldsymbol{\omega}\|^2, \quad (5)$$

here, the corresponding constraints are

$$|\boldsymbol{\omega} \cdot \boldsymbol{\varphi}(\mathbf{x}_i) + b - y_i| < \varepsilon \quad i = 1, 2, \dots, l. \quad (6)$$

Considering the permissible errors, two slack variables are introduced as follows:

$$\xi_i, \xi_i^* \geq 0 \quad i = 1, 2, \dots, l,$$

the optimization function is

$$\begin{aligned} \min & \frac{1}{2} \|\boldsymbol{\omega}\|^2 + \gamma \sum_{i=1}^l (\xi_i + \xi_i^*) \\ \text{s.t.} & \begin{cases} \boldsymbol{\omega} \cdot \boldsymbol{\varphi}(\mathbf{x}_i) + b - y_i \leq \xi_i^* + \varepsilon \\ y_i - \boldsymbol{\omega} \cdot \boldsymbol{\varphi}(\mathbf{x}_i) - b \leq \xi_i + \varepsilon \\ \xi_i, \xi_i^* \geq 0, \quad i = 1, 2, \dots, l \end{cases} \end{aligned} \quad (7)$$

where  $\gamma$  is a penalty coefficient.

For obtaining the solution of this quadratic program, the Lagrange function is adopted as

$$\begin{aligned}
L(\boldsymbol{\omega}, b, \mathbf{a}, \mathbf{a}^*) &= \min \frac{1}{2} \|\boldsymbol{\omega}\|^2 + \gamma \sum_{i=1}^l (\xi_i + \xi_i^*) \\
&\quad - \sum_{i=1}^l a_i (\xi_i + \varepsilon - y_i + \boldsymbol{\omega} \cdot \boldsymbol{\varphi}(\mathbf{x}_i) + b) \\
&\quad + \sum_{i=1}^l a_i^* (\xi_i^* + \varepsilon + y_i - \boldsymbol{\omega} \cdot \boldsymbol{\varphi}(\mathbf{x}_i) - b) \\
&\quad - \sum_{i=1}^l \eta_i (\xi_i + \xi_i^*),
\end{aligned} \tag{8}$$

where  $a_i, a_i^* \geq 0, i = 1, 2, \dots, l$ .

In the optimization process, a kernel function  $\psi(\mathbf{x}_i, \mathbf{x}_j)$  is applied to replacing the inner product  $\langle \boldsymbol{\varphi}(\mathbf{x}_i), \boldsymbol{\varphi}(\mathbf{x}_j) \rangle$  in higher dimensional space, where the Lagrange duality problem is expressed by

$$\begin{aligned}
\min_{a, a^*} &\left[ \frac{1}{2} \sum_{i, j=1}^l (a_i^* - a_i) (a_j^* - a_j) \psi(\mathbf{x}_i, \mathbf{x}_j) \right. \\
&\quad \left. + \varepsilon \sum_{i=1}^l (a_i^* - a_i) - \sum_{i=1}^l y_i (a_i^* - a_i) \right] \\
\text{s.t.} &\begin{cases} \sum_{i=1}^l (a_i^* - a_i) = 0 \\ 0 \leq a_i, a_i^* \leq \gamma; i = 1, 2, \dots, l \end{cases}
\end{aligned} \tag{9}$$

After getting the optimized solution  $\bar{a}_i, \bar{a}_i^*$  and  $\bar{b}$ , the regression estimating function (the response surface function of LSSVM) is

$$f(\mathbf{x}) = \sum_{\mathbf{x}_i \in \text{SV}} (\bar{a}_i - \bar{a}_i^*) \psi(\mathbf{x}, \mathbf{x}_i) + \bar{b}, \tag{10}$$

where SV is a set of support vectors for a given sample set,  $\mathbf{x}$  and  $\mathbf{x}_i$  are, respectively,

$$\mathbf{x} = [\mathbf{x}_1, \mathbf{x}_2, \dots, \mathbf{x}_l], \mathbf{x}_i = [x_{i1}, x_{i2}, \dots, x_{ir}]^T \tag{11}$$

in which  $i = 1, 2, \dots, l$ ,  $l$  the number of sample values, and  $r$  the number of random variables.

From the above analysis, the expression of LSSVM does not have relationship with the time, so that it is only suitable to the steady-state probabilistic analysis. Therefore, it is necessary to search for a novel approach to make LSSVM deal with dynamic probabilistic analysis issues.

### 3.2 Time-varying LSSVM

For the time-varying (dynamic or transient) probabilistic optimization problem, the response of each calculation is a stochastic process, which always results in the difficulty of LSSVM in solving the probabilistic analysis of complex structure. In the face of this situation, the conventional approaches are to fit a lot of response surface models in this time process and then select one reasonable response at one time point as the computational point of probabilistic analysis [2,28]. However, in all the loops of calculations for probabilistic analysis, it is difficult to ensure the selected computational point to be reasonable and feasible, so that the computational accuracy of probabilistic design is unworkable. To resolve this issue of LSSVM, this paper develops the T-LSSVM method which calculates a single extreme value rather than a series of dynamic output responses under different input samples within a time domain  $[0, T]$ . This process is equivalent to transform a stochastic process of output response into a random variable in each stochastic analysis. It can ensure that the random variable of output response is the most reasonable and effective, and then pledges analytical precision. In this subsection, T-LSSVM model is established based on these data for probabilistic analysis. The probabilistic analysis procedure with T-LSSVM is drawn as follows:

- (1) Establish the FE model of structure and select reasonable parameters such as dynamic load, constraint conditions, time domain.
- (2) Define the maximum output responses for each stochastic analysis within time domain by extracting the samples of input and output variables.
- (3) Fit the response surface function of T-LSSVM to these samples.
- (4) Accomplish structural dynamic probabilistic analysis by the response surface function of T-LSSVM.

Obviously, T-LSSVM is potential to reduce computing cost and enhance calculation efficiency. For the radial deformations probabilistic analyses of turbine disk, blade and casing, the maximum deformations are considered as the output responses of T-LSSVM during time domain  $[0, T]$ , because the time-varying deformation is secure in  $[0, T]$  as long as the maximum response is safe at the time point. Therefore, the establishment process of T-LSSVM model is shown in Fig. 3.

According to the basic thought of T-LSSVM in Fig. 3, the dataset with the maximum output response and input random variables is obtained through a number of stochastic analyses in time domain  $[0, T]$ . With the  $j$ th input samples  $x_j$ , the extremum of output response  $Y_i(t, x_i)$  is  $Y_{i,\max}(x_i)$  within the time domain  $[0, T]$ . The dataset  $\{Y_{i,\max}(x_i):i = 1, 2, \dots, l\}$  consisting of the maximum output responses is used to fit extremum response curve  $Y(x)$

$$Y(x) = f(x) = \{Y_{i,\max}(x_i):i = 1, 2, \dots, l\}. \quad (12)$$

where  $f(x)$  is a response surface function, called as T-LSSVM function. Based on the response surface function of LSSVM [Eq. (10)], the T-LSSVM function is constructed as

$$\begin{aligned}
Y(\mathbf{x}) &= \text{Max}_j [f(\mathbf{x}_j)] \\
&= \text{Max}_j \left\{ \sum_{\mathbf{x}_{ij} \in \text{SV}} (\bar{a}_{ij} - \bar{a}_{ij}^*) \psi(\mathbf{x}_j, \mathbf{x}_{ij}) + \bar{b}_j \right\}, \\
& \quad j \in N \tag{13}
\end{aligned}$$

where  $j = 1, 2, \dots, k$ ,  $k$  is the number of fitted response surface functions of T-LSSVM in one stochastic analysis process within  $[0, T]$ .

If the T-LSSVM function is applied to the dynamic probabilistic design of complex structure replacing FE model, this method is called as T-LSSVM method, which belongs to the global response surface method.

### 3.3 DC-T-LSSVM

*BTRRC* probabilistic analysis is a representative MOMD nonlinear dynamic probabilistic design so that it is difficult to implement its probabilistic analysis with high precision and acceptable efficiency. For the MOMD reliability analysis of complex mechanical assemble relationship, Bai and Fei developed the distributed collaborative strategy and distributed collaborative response surface method (DCRSVM) based on quadratic polynomial [2]. The strategy was validated to have fast speed with acceptable computational precision by the steady assembly reliability analysis of multiply components. Therefore, The DC-T-LSSVM is proposed for MOMD dynamic reliability analysis with respect to the distributed collaborative strategy and the presented T-LSSVM.

#### 3.3.1 Basic idea of DC-T-LSSVM

In the MOMD dynamic probabilistic analysis extended from T-LSSVM, an entire assemblage model, involving multiple system elements (sub-components) and multiple subjects, is firstly divided into several submodels, which are single-object single-disciplinary (SOSD) according to the structural features of complex machinery. Accompanying with the dividing process, the probabilistic analysis of the MOMD whole model is split into the corresponding probabilistic analyses of SOSD sub-models to structure distributed T-LSSVMs (SOSD T-LSSVMs) by the response features of SOSD probabilistic analyses. The extremum output responses of distributed T-LSSVMs are adopted as the input parameters of the collaborative T-LSSVMs to address the dynamic probabilistic analysis of complex machinery. This process is equivalent to integrate those sub-models to deal with the collaborative relationships among extremum output responses and further implement the MOMD dynamic probabilistic analysis. It is convenient for DCT-LSSVM to improve the computational precision and efficiency of machinery dynamic probabilistic analysis.

#### 3.3.2 Mathematical model

The mathematical model of DC-T-LSSVM is built for *BTRRC* dynamic probabilistic analysis based on the presented T-LSSVM. Assuming that an assemblage involves  $m$  objects and the analysis of each object refers to  $n$  disciplines, the complicated MOMD problem is converted to a series of simple SOSD problems. When  $\mathbf{X}^{pq}$  denotes the input samples of the  $q$ th subject in the  $p$ th



object, the output response  $Y^{pq}$  is

$$Y^{pq} = f(\mathbf{x}^{pq}), \quad p = 1, 2, \dots, m; \quad q = 1, 2, \dots, n \quad (14)$$

$$\mathbf{x}^{pq} = [x_1^{pq} \ x_2^{pq} \ \dots \ x_v^{pq}]^T \quad (15)$$

where  $v$  is the number of random variables of a single discipline. Hence, the response surface function of T-LSSVM for a single discipline from Eq. (15) is:

$$\begin{aligned} Y^{pq} &= f(\mathbf{x}^{pq}) = \text{Max}_j [f(\mathbf{x}_j^{pq})] \\ &= \text{Max}_j \left\{ \sum_{\mathbf{x}_{ij}^{pq} \in \text{SV}} (\bar{a}_{ij}^{pq} - \bar{a}_{ij}^{pq*}) \psi(\mathbf{x}_j^{pq}, \mathbf{x}_{ij}^{pq}) + \bar{b}_j^{pq} \right\} \end{aligned} \quad (16)$$

Equation (16) is the SOSD T-LSSVM model, where  $\bar{a}_{ij}^{pq}$ ,  $\bar{a}_{ij}^{pq*}$  and  $\bar{b}_j^{pq}$  are the optimal solutions of SOSD Lagrange function;  $\mathbf{x}_{ij}^{pq}$  is the  $i$ th sample of SOSD analysis.

The output responses  $\{Y^{pq}\}_{q=1}^n$  of all disciplines in each object are taken as the input variables  $\mathbf{x}^p$  of singleobject response surface model with multi-discipline, i.e.,

$$\mathbf{x}^p = \{Y^{pq}\}_{q=1}^n \quad (17)$$

The output response of single-object response surface model  $Y^{(p)}$  is

$$\begin{aligned} Y^p &= f(\mathbf{x}^p) = \text{Max}_j [f(\mathbf{x}_j^p)] \\ &= \text{Max}_j \left\{ \sum_{\mathbf{x}_{ij}^p \in \text{SV}} (\bar{a}_{ij}^p - \bar{a}_{ij}^{p*}) \psi(\mathbf{x}_j^p, \mathbf{x}_{ij}^p) + \bar{b}_j^p \right\}, \end{aligned} \quad (18)$$

This relationship is called single-object function of T-LSSVM, where  $\bar{a}_{ij}^p$ ,  $\bar{a}_{ij}^{p*}$  and  $\bar{b}_j^p$  are the optimal solutions of single-object multi-discipline (SOMD) Lagrange function;  $\mathbf{x}_{ij}^p$  is the  $i$ th sample of single-object analysis.

Similarly, the output responses  $\{Y^p\}_{p=1}^m$  of all objects are regarded as the input random variables  $\tilde{\mathbf{x}}$  of whole collaborative T-LSSVM model by

$$\tilde{\mathbf{x}} = \{Y^p\}_{p=1}^m \quad (19)$$

The whole T-LSSVM model  $\tilde{Y}$  is:

$$\begin{aligned}\tilde{Y} &= f(\tilde{\mathbf{x}}) = \text{Max}_j [f(\tilde{\mathbf{x}}_j)] \\ &= \text{Max}_j \left\{ \sum_{\tilde{\mathbf{x}}_{ij} \in \text{SV}} (\tilde{a}_{ij} - \tilde{a}_{ij}^*) \psi(\tilde{\mathbf{x}}_j, \tilde{\mathbf{x}}_{ij}) + \tilde{b}_j \right\}\end{aligned}\quad (20)$$

This relationship is called collaborative T-LSSVM model with MOMD, where  $\bar{a}_{ij}$ ,  $\bar{a}_{ij}^*$  and  $\bar{b}_j$  are the optimal solutions of MOMD Lagrange function; is the  $i$ th sample of MOMD analysis.

As shown by the above analysis, the T-LSSVM model [Eq. (13)] of system is decomposed into multiple T-LSSVMs (distributed T-LSSVM models) of sub-systems under different layers like Eqs. (16), (18) and (20). This method is called DC-T-LSSVM method. This method can be applied to MOMD dynamic probabilistic analysis.

### 3.3.3 Strengths of DC-T-LSSVM

From the above analysis, the DC-T-LSSVM is promising to improve the efficiency and accuracy of complex machinery dynamic probabilistic analysis by coordinating the distributed T-LSSVMs. The strengths are summarized as follows:

- (1) Automatic parallel calculations are available simultaneously on several computers to save computing time significantly;
- (2) Reduction of random variables of single model may shorten the computation time and alleviate computational task of fitting and simulating the TLSSVM model in dynamic probabilistic analysis;
- (3) The nonlinearity between input parameters and output responses is promising to be reasonably solved to improve the calculation accuracy by considering more factors and increase the simulation times;
- (4) The strengths of T-LSSVM ensure the efficiency and precision of DC-T-LSSVM in MOMD probabilistic analysis.

## 4. Basic thought of BTRRC probabilistic analysis

Probabilistic design mainly consists of reliability analysis and sensitivity analysis, which is an analysis technique of assessing the influential level of uncertain input parameters on the system output. Probabilistic analysis allows determining the extent to which uncertainties in the model affect the analysis results. It is feasible to avoid overdesign by the probabilistic methods while still ensuring the system safety. The probabilistic distribution characteristics of random parameters are helpful to improve BTRRC control in the development of advanced aeroengine.

### 4.1 BTRRC calculation and probabilistic analysis method

Assuming that  $Y_d(t)$ ,  $Y_b(t)$  and  $Y_c(t)$  are the radial deformations of turbine disk, turbine blade and turbine casing at time  $t$ , respectively, the variation  $\tau(t)$  of BTRRC could be calculated [3–6]

$$\tau(t) = Y_d(t) + Y_b(t) - Y_c(t) \quad (21)$$

Supposing that  $\delta$  is the HPT static tip clearance, the extremum response curve  $Y(t)$  of BTRRC can be achieved

$$Y(t) = \delta - \tau(t) = \delta - Y_d(t) - Y_b(t) + Y_c(t) \quad (22)$$

When  $Y(t)$  reaches the minimum  $Y$  at time  $t = t_0$ , from Eq. (22), the limit state function of BTRRC is

$$Y = \delta - Y_d - Y_b + Y_c \quad (23)$$

where  $Y_d$ ,  $Y_b$  and  $Y_c$  are the radial deformations of disk, blade and casing at time  $t_0$ , respectively.

As shown by Eq. (23),  $Y > 0$  can ensure the safety of BTRRC. When  $Y$  obeys the normal distribution, the variables in  $\mathbf{x}$  are independent and the mean and variance matrix of the variables in  $\mathbf{x}$  are  $\boldsymbol{\mu} = [\mu_d, \mu_b, \mu_c]$  and  $\boldsymbol{\sigma} = [\sigma_d, \sigma_b, \sigma_c]$

$$\begin{cases} E[Y] = \mu_Y(\mu_d, \mu_b, \mu_c, \sigma_d, \sigma_b, \sigma_c) \\ D[Y] = D_Y(\mu_d, \mu_b, \mu_c, \sigma_d, \sigma_b, \sigma_c) \end{cases} \quad (24)$$

here,  $E(\cdot)$  and  $D(\cdot)$  are the functions of mean value and variance function, respectively;  $\mu_Y$  and  $D_Y$  are the mean value and variance performance functions of the limit state function  $Y$  [Eq. (23)].  $i, j = 1, 2, \dots, r$ ;  $r$  is the number of random variables.

The reliability index  $\beta$  and reliability degree  $R$  of output response  $Y$  [28] are

$$\begin{cases} R = \Phi(\beta) \\ \beta = \frac{\mu_Y}{\sqrt{D_Y}} \end{cases} \quad (25)$$

in which  $\Phi(\cdot)$  is the cumulative normal distribution function.

For MOMD distributed collaborative sensitivity analysis, the detailed analysis steps are depicted as follows:

Firstly, the sensitivities and probabilities of the original variables of the  $q$ th subject in the  $p$ th object impacting the SOSD output response  $Y^{pq}$  are calculated by.

$$\begin{cases} \mathbf{S}^{pq} = [S_1^{pq}, S_2^{pq}, \dots, S_v^{pq}] \\ \mathbf{P}^{pq} = [P_1^{pq}, P_2^{pq}, \dots, P_v^{pq}] \end{cases} \quad (26)$$

Similarly, for the all output responses  $\{Y^{pq}\}_{p=1}^n$  of  $p$ th object affecting the output response  $Y^p$  (SOMD) and all output responses  $\{Y^p\}_{p=1}^m$  of objects influencing the whole output response  $Y$  (MOMD), their sensitivities and probabilities are, respectively,

$$\begin{cases} \mathbf{S}^p = [S_1^p, S_2^p, \dots, S_n^p] \\ \mathbf{P}^p = [P_1^p, P_2^p, \dots, P_n^p] \end{cases} \quad (27)$$

$$\begin{cases} \mathbf{S}' = [S_1, S_2, \dots, S_m] \\ \mathbf{P}' = [P_1, P_2, \dots, P_m] \end{cases} \quad (28)$$

where S and P indicate the sensitivity and the probability (reliability degree), respectively.

Secondly, according to the conditional probability analysis thought, the sensitivity and probability of the  $i$ th original variables impacting the whole output response Y of MOMD are gained

$$\begin{cases} \tilde{S}_i^{pq} = S_i^{pq} \cdot S_s^p \cdot S_t \\ \tilde{P}_i^{pq} = P_i^{pq} \cdot P_s^p \cdot P_t \end{cases} \quad (29)$$

where  $i = 1, 2, \dots, v$ ;  $s = 1, 2, \dots, n$ ; and  $t = 1, 2, \dots, m$ .

Lastly, the above steps are not proceeded repeatedly until all sensitivities and probabilities of original variables are obtained. For the same variables, the sensitivities and probabilities are superposed in different objects and disciplines. The sensitivity S and probability P of original variables influencing the overall output response Y are gained by

$$\begin{cases} \mathbf{S} = [S_1, S_2, \dots, S_r] \\ \mathbf{P} = [P_1, P_2, \dots, P_r] \end{cases} \quad (30)$$

where r is the number of original variables.

## 4.2 Essential process

The BTRRC of an aeroengine HPT is used to verify DC-T-LSSVM proposed in this paper. The flight profile and computing range in Fig. 4 were selected from a sequence (start-idling-takeoff-climb-cruise) of aeroengine operating points [3,7]. Twelve operating points were taken as the computing points. The fundamental idea of BTRRC dynamic probabilistic analysis is that the BTRRC analysis is divided into the radial deformation analyses of disk, blade and casing. This analysis process is shown in Fig. 5.

## 5. Deterministic analyses

### 5.1 FE mode

In this paper, the BTRRC of an aeroengine high-pressure turbine was selected to complete nonlinear dynamic MOMD probabilistic analysis with the proposed DC-T-LSSVM. According to Fig. 1, the turbine blisk was reduced to build the integrated FE model as shown in Fig. 6a. The structure of turbine casing was simplified to establish a cylinder FE model as shown in Fig. 6b. Based on the basic thought of distributed collaborative strategy, the whole turbine blisk was divided into turbine disk and turbine blade. Due to the axisymmetric bladed disk and casing model, the shaft section FE models (Fig. 6c, e) of turbine disk and turbine casing were selected as the objects of study, and the FE model (Fig. 6d) of

single blade was regarded as the object of study for the sake of reducing computational loads under keeping the computing precision.

In disk FE model, the mortises and cooling holes were ignored to concentrate on BTRRC analysis and reduce the complexity of the analysis of radial deformations. The loads and constraint conditions on the surface of turbine disk are axisymmetric and air-cooled. The temperatures of A1, A2, A3, B1, B2 and B3 on disk model were computed according to the boundary conditions of heat transfer [3–5,9–11]. In blade FE model, the tenons of turbine blade was simplified and reassigned on the disk model. In casing FE model, the bushing ring of casing is a sensitive element because its expansion and contraction cause casing's radial deformation and then change the blade-tip clearance. Therefore, only the bushing ring was analyzed, and its axial section was studied. The surface coefficients of heat transfer of three objects were calculated by the heat transfer characteristics in [3–5,7–11].

## 5.2 Selection of random variables

The material property and dynamic loads possess conspicuous randomness and act a major impact on the BTRRC of aeroengine. For the BTRRC dynamic probabilistic analysis, the essential factors (rotor speed, gas temperature, thermal conductivity, expansion coefficients, surface coefficients of heat transfer and material density) are selected in Table 1, by the extremum selection method which is effective for selecting the nonlinear or/and dynamic variables [35]. The variables are assumed to be reciprocally independent and obey a normal distribution.

## 5.3 Dynamic deterministic analysis

In the selected parameters of material property in Table 1, thermal conductivity, expansion coefficients, surface coefficients of heat transfer and material density are nonlinear factors because they nonlinearly vary with temperature. Wherein, the nonlinearity attributes of thermal conductivity  $\lambda$  and expansion coefficient  $\kappa$  for three components (disk, blade and casing) were selected as shown in Table 2. Besides, the selected loads in Table 1, rotor speed  $\omega$ , gas temperature  $T$  are nonlinear dynamic parameters which nonlinear change with time, as shown Fig. 4. With respect to the nonlinear and/or dynamic parameters, the radial deformations of objects were analyzed comprising of thermal analysis and structural analysis, respectively, by importing the means of variables in Table 1 into the FE models. It is obvious that the analysis is nonlinear dynamic due to the nonlinearity and dynamics of material parameters and loads. In this analysis, a thermal analysis was performed at a time point, and then, the gained thermal stress is applied to structure for obtaining the dynamic analysis results considering the effect of the rotational speed and the nonlinear factors at this time point. The nonlinear relationship exists between variations of objects and BTRRC(also including their stress and stains generated in the process of analysis) and the input variables. The radial deformation distributions of output responses when the maximum output responses reach at the peak are shown in Fig. 7.

The analytical results show that the maximum radial deformations of disk, blade and casing are  $1.369 \times 10^{-3}$  m,  $1.291 \times 10^{-3}$  m and  $8.699 \times 10^{-4}$  m at  $t = 181.2$  s, respectively. Meanwhile, the minimum BTRRC is  $2.009 \times 10^{-4}$  m and the maximum radial deformation of BTRRC is  $1.7901 \times 10^{-3}$  m when the blade-tip radial static clearance reserved is  $\delta = 2 \times 10^{-3}$  m.

## 6. Dynamic probabilistic analyses of three objects

In this section, the distributed T-LSSVM models and distribution characteristics of disk, blade and casing radial deformations are obtained through the dynamic probabilistic analyses with DC-T-LSSVM.

### 6.1 Establishment of distributed time-varying LSSVM

After inputting the statistical characteristics of random variables into the FE models, based on MC method, three data sets containing 50 groups of samples for disk, blade and casing are extracted, respectively, to fit the distributed T-LSSVM models by using ANSYS software. These simulation numbers are effective and sufficient to fit the corresponding T-LSSVM models. The relationship nephograms between three output responses and partial input random variables, respectively, is shown in Fig. 8.

### 6.2 Distribution characteristics of output responses

Three fitted distributed T-LSSVM models were simulated at 10,000 times by MC method to fulfill the dynamic (time-varying) probabilistic analyses for three FE models. The distribution characteristics of  $Y_d$ ,  $Y_b$  and  $Y_c$  are shown in Table 3.

### 6.3 Sensitivity analysis

The sensitivity analysis is used to analyze the effecting significance of input random variables on the stability of output parameters to decide which parameters greatly impact the system failure and then provide a guidance for the design of radial deformations. Through the simulation of three objects, the sensitivity (Sen) and affecting probability (Pa) of the variables are acquired in Fig. 9.

In Fig. 9, the positive sensitivity illustrates that the input parameters show the positive influence on the random output variables, vice versa. By the implications from Fig. 9, the conclusions are drawn as follows:

- (1) For the radial deformation of the disk, it is obvious that the rotor speed  $\omega$  is the most important factor and plays a leading role in the variation of BTRRC as the sensitivity (0.88124) and impact probability (0.6663) are the largest among the considered factors. In addition, the gas temperature  $T$  is also a main factor with the sensitivity 0.43565 and probability 0.3291, while the influences from the other factors are relatively weak.
- (2) Between the two essential factors (gas temperature  $T$  and rotor speed  $\omega$ ) of blade radial deformation dynamic probabilistic analysis, the impacting probability  $T$  (0.623) is greater than the  $\omega$  (0.3384). The reason leading to the result may be that the high-temperature creep behavior of the material mainly impacts on turbine blade radial deformation during aeroengine operation rather than the centrifugal stress for the relatively small-sized blade, while other factors perform hardly influence on blade radial deformation.
- (3) From the casing radial deformation, the gas temperature  $T$  is illustrated to be the unique factor (also may be seen from Fig. 8c) because of the probability of 0.9642, while other factors perform hardly influence on the blade radial deformation.

The above results are consistent with empirical practices, which may be provided as a foundation to design and control of BTRRC.

## 7. Dynamic probabilistic analysis of blade-tip radial clearance

In this section, the output responses of the distributed T-LSSVMs were regarded as the input parameters for the dynamic probabilistic analysis of the BTRRC. Eqs. (21)–(23) were treated as the collaborative TLSSVMs to accomplish the MOMD dynamic probabilistic analysis of BTRRC.

### 7.1 Reliability analysis

The collaborative T-LSSVMs were simulated for 10,000 times by MC method with Latin Hypercube sampling method. The simulation history and histogram of  $\tau$  and the reliability analysis results are shown in Fig. 10 and Table 4.

As demonstrated in Table 4 and Fig. 10, it is feasible to acquire the failure probability and reliability characteristics of the output response  $Y$  (BTRRC), which is also a Gaussian distribution.  $\delta = 1.82 \times 10^{-3}$  m (in Fig. 10b) is suggested as the static clearance since  $R = 99.9\%$  satisfies basically the design requirement with respect to the reliability and efficiency of gas turbine synthetically.

### 7.2 Sensitivity analysis for BTRRC

Through BTRRC sensitivity analysis based on Eqs. (26)–(30), the sensitivities and probabilities of  $Y_d$ ,  $Y_b$ ,  $Y_c$  and the original variables are gained, respectively, which are shown in Table 5 and Fig. 11 (ignoring the variables with  $P_a < 0.001$ ).

It is revealed in Table 5 and Fig. 11 that the  $Y_d$ ,  $Y_b$  and  $Y_c$  are very important on BTRRC. The sensitivity degree of  $Y_d$  and  $Y_b$  is larger than zero, while the sensitivity degree of  $Y_c$  is smaller than zero. The results show that the BTRRC becomes large when  $Y_d$  and  $Y_b$  increase and  $Y_c$  reduces. Therefore,  $Y_d$  and  $Y_b$  perform the positive effects on the BTRRC, while  $Y_c$  has the negative impact. In addition, it is shown in Fig. 11 that  $\omega$  and  $T$  are the most important factors and thus should be considered with priority in designing the BTRRC. The expansion coefficients and the surface coefficients of heat transfer are relatively less important on BTRRC.

### 7.3 Comparison of methods

In order to support the validity and feasibility of the proposed DC-T-LSSVM, the results of BTRRC dynamic probabilistic analysis were compared with these of MC method, T-LSSVM and DCRSM in [2] under different times of simulations based on the variables in Table 1 and the same hardware conditions. In this analysis process, the DC-T-LSSVM and DCRSM adopt the automatic parallel computation in three computers, while the T-LSSVM and MC methods are implemented by the nonlinear dynamic analysis of whole BTRRC assemblage. The analysis results are listed in Table 6 and Fig. 12 under different number of simulations. In Table 6, the sample number is the number of samples required for fitting the corresponding response surface model, and the time of one calculation denotes one steady-state analysis in one transient analysis (ignoring the computing time larger than  $10^6$  s in Table 6). In Fig. 12, the reliability degree and precision of BTRRC at  $\delta = 1.82 \times 10^{-3}$  m for T-LSSVM, DCRSM and DC-T-LSSVM under different simulation number were calculated relative to reliability degree (0.999) of MC method at  $10^3$  times simulations.

From Table 6 and Fig. 12, some phenomena are drawn as follows:

As shown in Table 6, (1) for the fitting time of response surface models, the proposed DC-T-LSSVM ( $1.364 \times 10^4$  s) is far less than T-LSSVM ( $3.791 \times 10^5$  s) and larger than DCRSM ( $1.711 \times 10^3$  s). The reason is that (i) for the former, the whole BTRRC analysis with T-LSSVM includes much more input variable and requires much more fitting samples (381 groups), so that the computational loads is very large on one computer relative to DC-T-LSSVM (only requiring 30 groups); (ii) for the latter, the BTRRC analysis with DCRSM is steady state by regarding one dangerous point as the analysis point, while the analysis with DC-T-LSSVM is transient with respect to hundreds times of calculations in time domain  $[0, 215$  s] resulting in the large computational loads. However, (iii) the once computing time

(11.367 s) of DC-T-LSSVM is less than DCRSM for the LSSVM holding higher computing speed and less fitting samples. Moreover, (vi) less fitting samples (30 groups) required insure the higher fitting speed for DC-T-LSSVM relative to the DCRSM with 49 groups; (2) for the simulation time of four methods, (i) for the simulations of BTRRC, the MC method is unacceptable because the simulation time is too long (over  $10^6$  s) when the simulation is more than  $10^3$  times; (ii) the DC-T-LSSVM method is fastest under different simulation number in the three response surface methods for the rapidity of LSSVM in computation; (3) for DC-T-LSSVM, the strengths of fairly affordable computing cost and high efficiency become more remarkable with the increasing simulation times.

On the aspect of computing precision from Fig. 12, it is unveiled that DC-T-LSSVM is more precise than T-LSSVM and DCRSM, and is fairly equal to the accuracy of MC method at  $10^6$  times simulations. In addition, the reliability degree and precision of the three methods are improved with the increase in simulation times.

In summary, by the example of determining the BTRRC, the presented DC-T-LSSVM is verified to be an effective and feasible methodology with high precision and high efficiency in the dynamic probabilistic analysis of complex machinery. In the probabilistic analysis of BTRRC, the considered important parameters in this study mainly pledge the effectiveness of the results, although additional factors, such as mass eccentricity, substructure interaction, were not considered, because additional factors have less influence than the considered important parameters on the variation of BTRRC and the corresponding objects.

## 8. Conclusions

Distributed collaborative time-varying least squares support vector machine method (DC-T-LSSVM) with high accuracy and high efficiency was developed and applied to the dynamic probabilistic analysis of blade-tip radial clearance of high-pressure turbine at different point and different time with consideration of multiple physical parameters including nonlinear and dynamic variables. Through this investigation, the reasonable blade-tip radial clearance is gained and the DC-T-LSSVM is supported to be effective and feasible. These efforts provide a basis for collaborating additional details to improve the accuracy of BTRRC probabilistic analysis and develop a high performance and high reliability of aeroengine. Some conclusions are drawn as follows:

- 1) By the comparison of the proposed DC-T-LSSVM with MC method, T-LSSVM and DCRSM, it is demonstrated that the DC-T-LSSVM performs the strengths of the highest precision and highest efficiency, implies higher potential computational efficiency with the increasing simulation times for BTRRC dynamic probabilistic analysis, and provides an advisable reference for the BTRRC design, which enrich mechanical probabilistic analysis theory and method.
- 2) Through the dynamic probabilistic analysis of the turbine components and the BTRRC, the reliability, distribution characteristics and failure probability are obtained. Moreover,  $\delta=1.82 \times 10^{-3}$  m is suggested catering for the design requirement under comprehensively considering the reliability and efficiency of aeroengine. But it is only a important reference and guidance in blade-tip clearance design for designers and engineers.
- 3) From the sensitive analysis of BTRRC, the radial deformations ( $Y_d$ ,  $Y_b$  and  $Y_c$ ) and the original variables ( $\omega$ ,  $T$ ,  $\kappa$  and  $\alpha$ ) are influential parameters on BTRRC and worth of being considered in the regulation and design of BTRRC.  $Y_d$  and  $Y_b$  perform the positive effects on the BTRRC, while  $Y_c$  has the negative impact.



- 4) The distribution features and response surface nephograms of three variables for the radial deformation of each assemble object of BTRRC and the probabilistic distributions and effect levels of input random variables on the deformation of each object are obtained.
- 5) In the light of this study, additional factors such as gasdynamics and vibration mechanics should be focused on to enhance BTRRC design for further applications and usefulness of the DC-T-LSSVM.

Discrepancies do exist. Most deviations from expected response are likely to be attributed to incomplete factors considered. It is not the purpose of this paper to incorporate completely the details contained therein. However, this study provides a basis for collaborating additional details, which could improve the accuracy of BTRRC probabilistic analysis and develop a high performance and high reliability of gas turbo- machine like an aeroengine in future. In the light of this study and the questions raised, the following issues have to be resolved in the coming work:

- 1) Different DCRSMs based on different RSMs, such as quadratic function, support vector machine model, artificial neural network model, should be established by the features of different objects and different disciplines to improve the validity and precision of dynamic probabilistic analysis for complex machinery.
- 2) To enhance the quality of BTRRC dynamic probabilistic analysis, more accurate FE models and more reasonable analysis techniques should be adopted in future.
- 3) Additional factors (substructure interaction, gasdynamics, vibration mechanics, and so forth) should be cared to improve BTRRC dynamic probabilistic design.

Advanced work is to involve elaborate investigations on documented parameters and mechanisms. The current model is to be refined and validated by experiment and test data in order to assess the usefulness for BTRRC probabilistic analysis and design.

## **Acknowledgments**

The paper is co-supported by the National Natural Science Foundation of China (Grant No. 51275024), General Research Grant from Hong Kong SAR Government (Grant No. 514013(B-Q39B)), the Foundation of Hong Kong Scholars Program (Grant Nos. G-YZ290 and XJ2015002) and the Funding of Hong Kong Scholars Program (XJ2015002). The authors would like to thank them.

## References

1. Gole, N., Kumar, A., Narasimhan, V.: Health risk assessment and prognosis of gas turbine blades by simulation and statistical methods [C]. In: Canadian Conference on Electrical and Computer Engineering, pp. 1087–1092. Niagara Falls, Canada (2008)
2. Bai, G.C., Fei, C.W.: Distributed collaborative response surface method for mechanical dynamic assembly reliability design. *Chin. J. Mech. Eng.* 26, 1160–1168 (2013)
3. Lattime, S.B., Steinetz, B.M.: Turbine engine clearance control systems: current practices and future directions. *J. Propuls. Power* 20, 302–311 (2004)
4. Lattime, S.B., Steinetz, B.M., Robbie, M.G.: Test rig for evaluating active turbine blade tip clearance control concepts. *J. Propuls. Power* 21, 552–563 (2005)
5. NNSA Glenn Research Center: HTP Clearance Control, NASA/CR-2005-213970 (2005)
6. Jia, B.H., Zhang, X.D.: Study on effect of rotor vibration on tip clearance variation and fast active control of tip clearance. *Adv. Mater. Res.* 139–141, 2469–2472 (2010)
7. Annette, E.N., Christoph, W.M., Stehan, S.: Modeling and validation of the thermal effects on gas turbine transients. *J. Eng. Gas Turbines Power* 127, 564–572 (2005)
8. Forssell, L.S.: Flight clearance analysis using global nonlinear optimisation-based search algorithms. In: AIAA Guidance, Navigation, and Control Conference and Exhibit, pp. 1–8. Austin, Texas (2003)
9. Lattime, S.B., Steinetz, B.M.: Turbine engine clearance control systems: current practices and future directions. NASA/TM-2002-211794 (2002)
10. Kypuros, J.A., Melcher, K.J.: A reduced model for prediction of thermal and rotational effects on turbine tip clearance. NASA/TM-2003-212226 (2003)
11. Annette, E.N., Christoph, W.M., Stephan, S.: Modelling and validation of the thermal effects on gas turbine transients. *J. Eng. Gas Turbines Power* 127, 564–572 (2005)
12. Hu, D.Y., Wang, R.Q., Tao, Z.: Probabilistic design for turbine disk at high temperature. *Aircr. Eng. Aerosp. Technol.* 83, 199–207 (2011)
13. Reed, D.A.: Reliability of multi-component assemblages. *Reliab. Eng. Syst. Saf.* 27(2), 167–178 (1990)
14. Li, D.M., Zhang, X.M., Guan, Y.S.: Multi-objective topology optimization of thermo-mechanical compliant mechanisms. *Chin. J. Mech. Eng.* 24, 1123–1129 (2011)
15. Lv, Q., Low, B.K.: Probabilistic analysis of underground rock excavations using response surface method and SORM. *Comput. Geotech.* 38, 1008–1021 (2011)
16. Murat, E.K., Hasan, B.B., Aledar, B.: Probabilistic nonlinear analysis of CFR dams by MCS using response surface method. *Appl. Math. Model.* 35, 2752–2770 (2011)
17. Fitzpatrick, C.K., Baldwin, M.A., Rullkoetter, P.J., et al.: Combined probabilistic and principal component analysis approach for multivariate sensitivity evaluation and application to implanted patellofemoral mechanics. *J. Biomech.* 44, 13–21 (2011)
18. Alessandro, Z., Michele, B., Andrea, D.A., et al.: Probabilistic analysis for design assessment of continuous steel concrete composite girders. *J. Constr. Steel Res.* 66, 897–905 (2010)
19. Toshiya, N., Kenji, F.: Probabilistic transient thermal analysis of an atmospheric reentry vehicle structure. *Aerosp. Sci. Technol.* 10, 346–354 (2006)

20. Sung, E.C.: Probabilistic stability analyses of slopes using the ANN-based response surface. *Comput. Geotechn.* 36, 787–797 (2009)
21. Eom, Y.S., Yoo, K.S., Park, J.Y.: Reliability-based topology optimization using a standard response surface method for three-dimensional structures. *Struct. Multidiscipl. Optim.* 43, 287–295 (2011)
22. Zhang, C.Y., Bai, G.C.: Extremum response surface method of reliability analysis on two-link flexible robot manipulator. *J. Cent. South Univ.* 19, 101–107 (2012)
23. Pellissetti, M.F., Schueller, G.I., Pradlwarter, H.J., et al.: Reliability analysis of spacecraft structures under static and dynamic loading. *Comput. Struct.* 84(21), 1313–1325 (2006)
24. Huang, Z.J., Wang, C.G., Chen, J.: Optimal design of aero-engine turbine disc based on Kriging surrogate models. *Comput. Struct.* 89, 27–37 (2011)
25. Tan, X.H., Bi, W.H., Hou, X.L., et al.: Reliability analysis using radial basis function networks and support vector machines. *Comput. Geotech.* 38, 178–186 (2011)
26. Guo, Z.W., Bai, G.C.: Application of least squares support vector machine for regression to reliability analysis. *Chin. J. Aeronaut.* 22, 160–166 (2009)
27. Fei, C.W., Bai, G.C.: Nonlinear dynamic probabilistic analysis for turbine casing radial deformation using extremum response surface method based on support vector machine. *J. Comput. Nonlinear Dyn.* 8, 041004 (2013)
28. Fei, C.W., Bai, G.C.: Distributed collaborative probabilistic design for turbine blade-tip radial running clearance using support vector machine of regression. *Mech. Syst. Signal Process.* 49, 196–208 (2014)
29. Basudhar, A., Missoum, S.: Adaptive explicit decision functions for probabilistic design and optimization using support vector machines. *Comput. Struct.* 86, 1904–1917 (2008)
30. Tian, J., Gu, H.: Anomaly detection combining one-class SVMs and particle swarm optimization algorithms. *Nonlinear Dyn.* 61, 303–310 (2010)
31. Tian, J., Gu, H., Gao, C.Y.: Local density one-class support vector machines for anomaly detection. *Nonlinear Dyn.* 64, 127–130 (2011)
32. Guo, Z.K., Guan, X.P.: Nonlinear generalized predictive control based on online least squares support vector machines. *Nonlinear Dyn.* 79, 1163–1168 (2015)
33. Fei, C.W., Bai, G.C.: Distributed collaborative extremum response surface method for mechanical dynamic assembly reliability analysis. *J. Cent. South Univ.* 20, 2414–2422 (2013)
34. Fei, C.W., Bai, G.C.: Wavelet correlation feature scale entropy and fuzzy support vector machine approach for aero-engine whole-body vibration fault diagnosis. *Shock Vib.* 20, 341–349 (2013)
35. Fei, C.W., Bai, G.C.: Study on extremum selection method of random variable for nonlinear dynamic reliability analysis. *Propuls. Power Res.* 1, 58–63 (2012)

## Figures

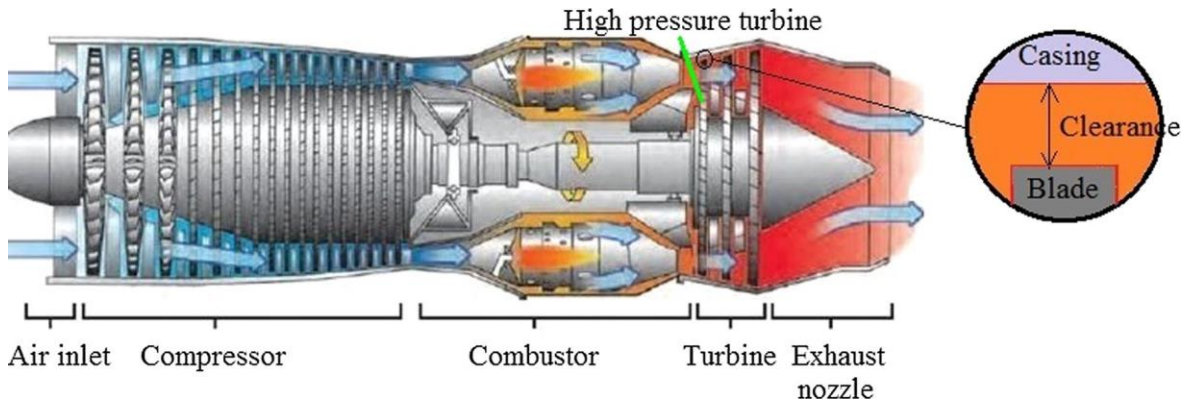


Fig. 1 BTRRC sketch of an aeroengine high-pressure turbine

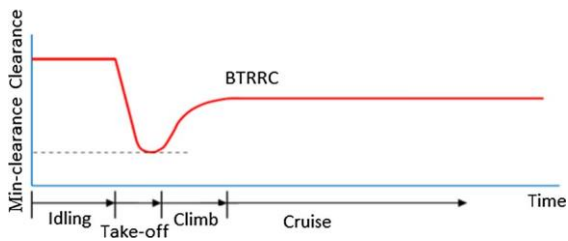


Fig. 2 Change curve of BTRRC for an aeroengine

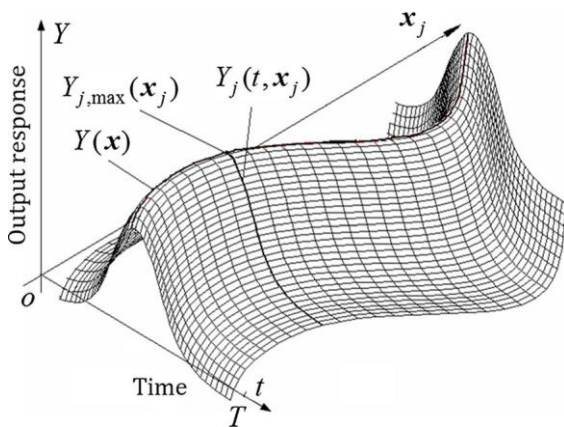


Fig. 3 Schematic diagram of T-LSSVM

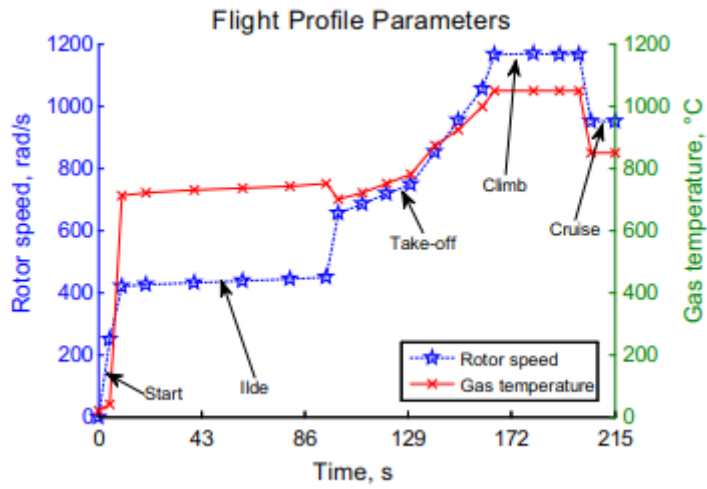


Fig. 4 Load spectra from an aeroengine

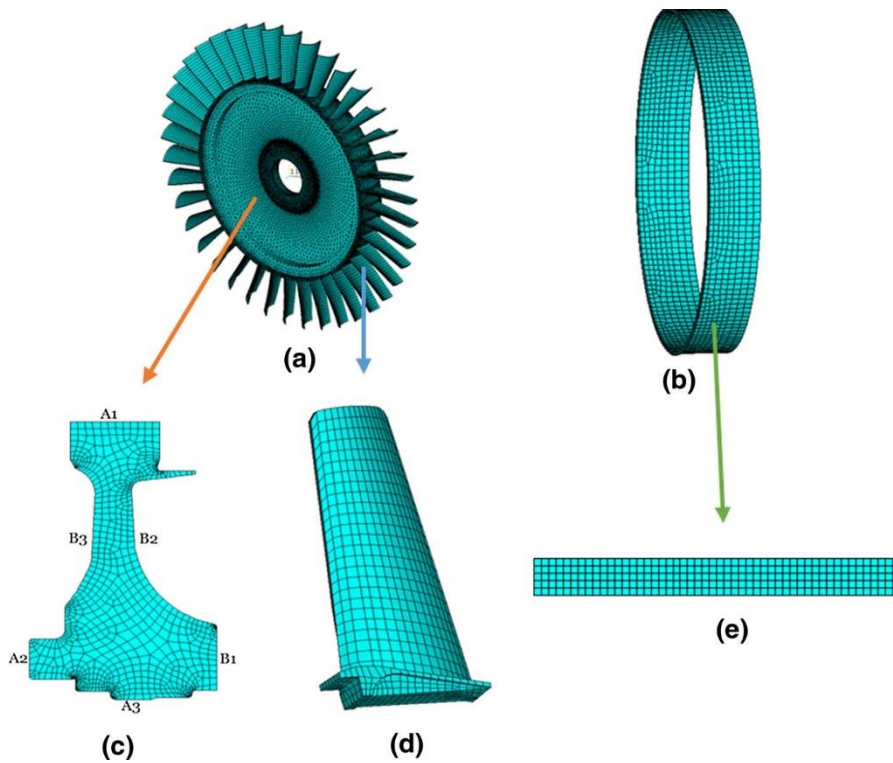
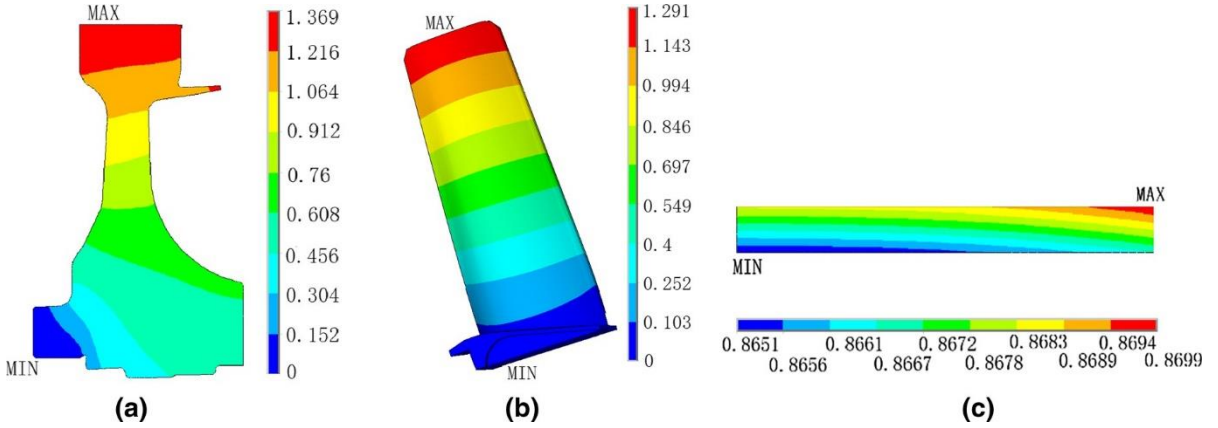
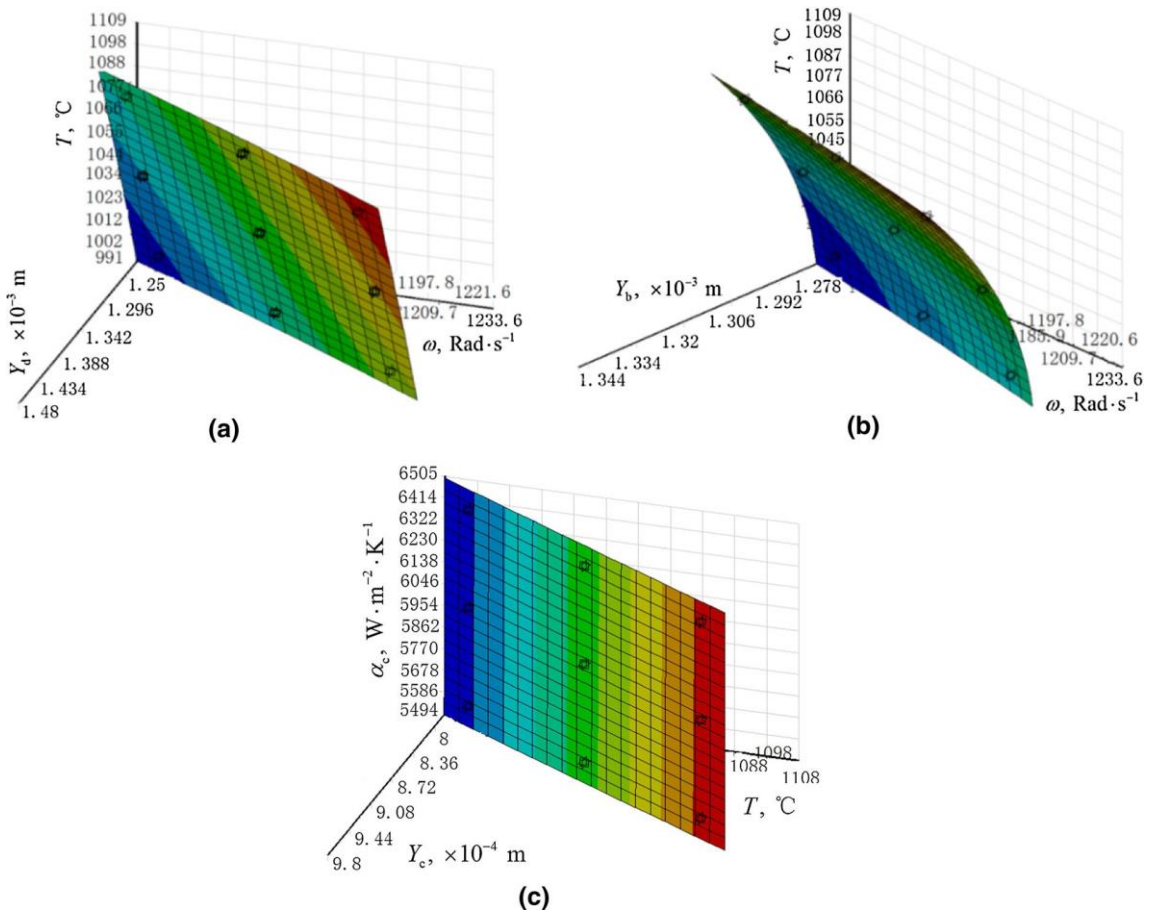


Fig. 6 Decomposition process of FE models: **a** whole turbine bladed disk; **b** whole turbine casing; **c** turbine disk; **d** turbine blade; **e** turbine casing



**Fig. 7** Distributions of maximum radial deformations ( $\times 10^{-3}$  m) of **a** turbine disk, **b** turbine blade and **c** turbine casing



**Fig. 8** Relationship nephograms between three output responses and partial variables: **a** Relationship between  $Y_d$  and  $T$ ,  $\omega$ ; **b** Relationship between  $Y_b$  and  $T$ ,  $\omega$ ; **c** Relationship between  $Y_c$  and  $T$ ,  $\alpha_c$

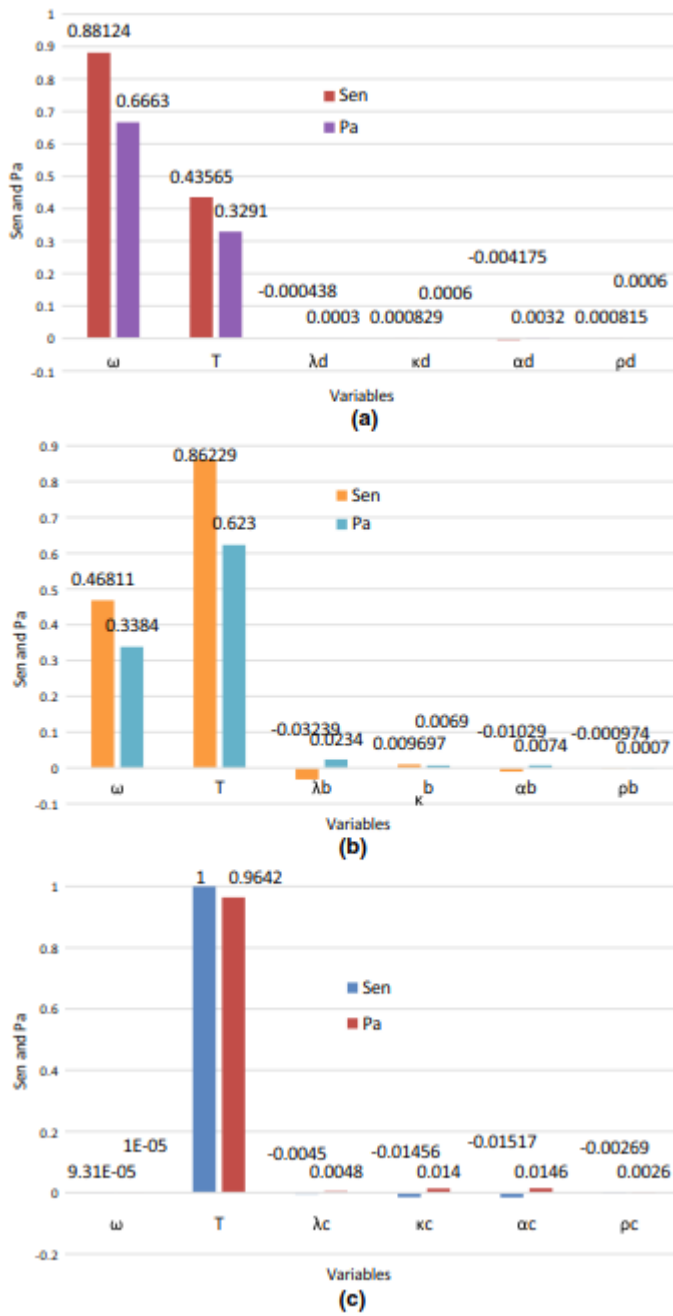


Fig. 9 Sensitivity analytical results of random variables for a turbine disk, b turbine blade and c turbine casing

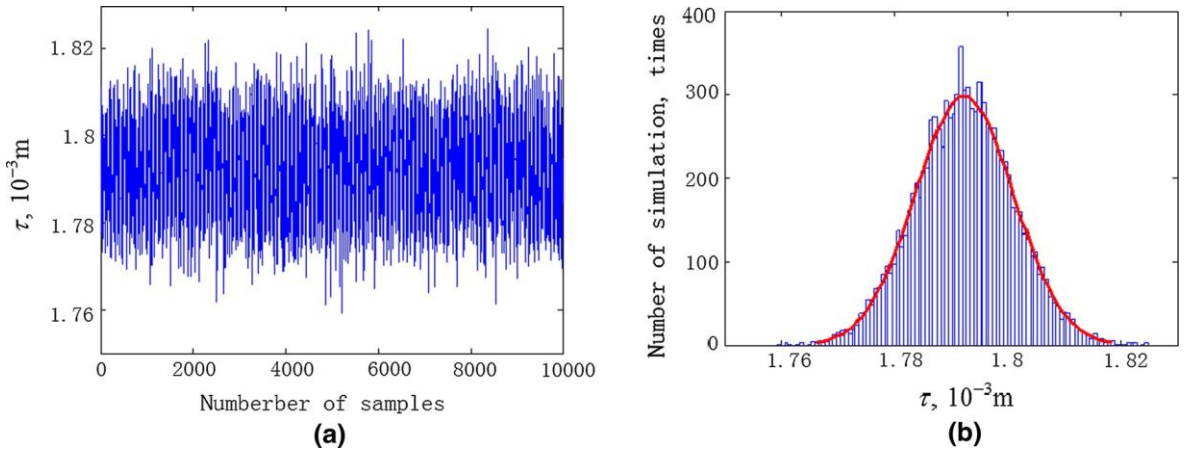


Fig. 10 Output responses of BTRRC reliability analysis: **a** Simulation history of  $\tau$ ; **b** distribution histogram of  $\tau$

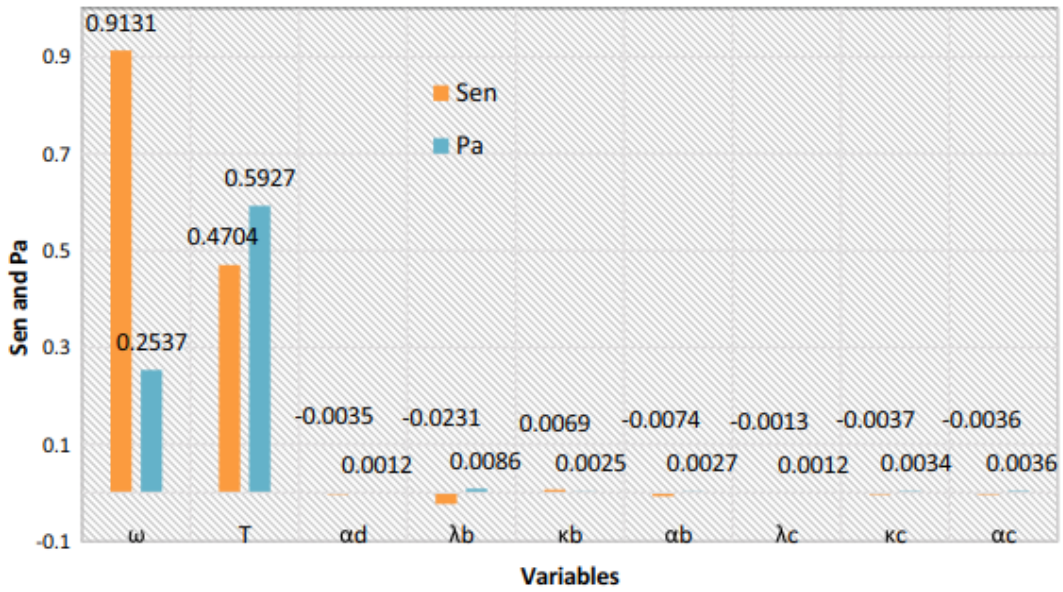


Fig. 11 Sensitivity analysis results of original variables on BTRRC ( $P_a > 0.001$ )



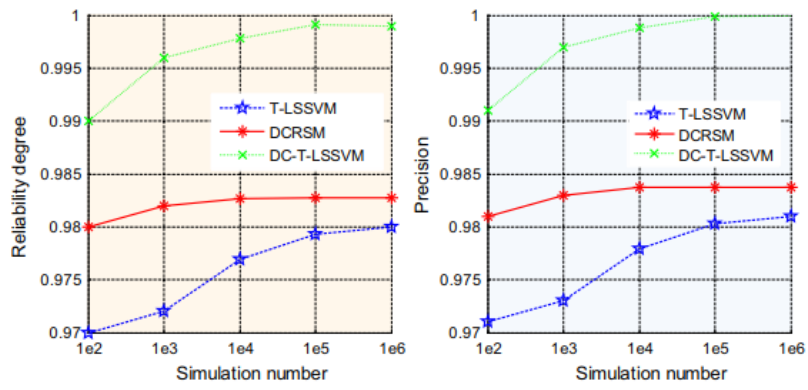


Fig. 12 Reliability degree and precision of three methods under different simulations

## Tables

Variable type	Disk			Blade			Casing		
	Variable	Mean $\mu$	Standard deviation	Variable	Mean $\mu$	Standard deviation	Variable	Mean $\mu$	Standard deviation
Rotor speed (Rad s <sup>-1</sup> )	$\omega$	1168	34	$\omega$	1168	34	$\omega$	1168	34
Gas temperature (°C)	$T$	1050	31	$T$	1050	31	$T$	1050	31
Thermal conductivity (W/(m °C))	$\lambda_d$	28	0.83	$\lambda_b$	27.8	0.83	$\lambda_c$	27.8	0.83
Expansion coefficients (10 <sup>-5</sup> °C)	$\kappa_d$	1.6	0.048	$\kappa_b$	1.6	0.048	$\kappa_c$	13	0.4
Surface coefficients of heat transfer (W/m <sup>2</sup> K)	$\alpha_d$	1500	45	$\alpha_b$	11756	353	$\alpha_c$	6000	180
Density (kg m <sup>-3</sup> )	$\rho_d$	8210	246	$\rho_b$	8210	246	$\rho_c$	8400	252

**Table 1** Random variables for BTRRC dynamic probabilistic analysis

Objects	Temperature, $T$ , (°C)	100	200	300	400	500	600	700	800	900
Disk	Thermal conductivity, $\lambda$ (W m <sup>-1</sup> °C <sup>-1</sup> )	10.5	14.2	17.2	18.8	20.5	22.6	24.3	26.0	27.2
	Expansion coefficient, $\kappa$ (10 <sup>-5</sup> °C)	1.16	1.23	1.26	1.32	1.36	1.41	1.47	1.51	1.57
Blade	Thermal conductivity, $\lambda$ (W m <sup>-1</sup> °C <sup>-1</sup> )	12.2	13.8	16.3	18.6	20.1	21.8	23.9	26.2	27.8
	Expansion coefficient, $\kappa$ (10 <sup>-5</sup> °C)	1.16	1.23	1.24	1.33	1.35	1.44	1.51	1.57	1.65
Casing	Thermal conductivity, $\lambda$ (W m <sup>-1</sup> °C <sup>-1</sup> )	14.6	16.6	18.0	19.4	20.8	22.4	23.8	25.0	26.6
	Expansion coefficient, $\kappa$ (10 <sup>-5</sup> °C)	1.28	1.35	1.43	1.5	1.55	1.61	1.7	1.75	1.8

**Table 2** Heat conductivities and linear expansion coefficients under different temperature (reference 20 °C)

**Table 3** Distribution characteristics of maximum radial deformations of three objects

Characteristic	$Y_d$	$Y_b$	$Y_c$
Mean ( $\times 10^{-3}$ m)	1.3671	1.2902	0.86491
Standard deviation ( $\times 10^{-5}$ m)	3.218	0.9335	3.2816
Distribution	Normal	Normal	Normal

**Table 3** Distribution characteristics of maximum radial deformations of three objects

	Failure number	Failure probability	Reliability	Mean ( $\times 10^{-3}$ m)	Standard deviation ( $\times 10^{-3}$ m)	Distribution	Computational time (s)
Maximum deformation $\tau$	–	–	–	1.79236	0.0087	Normal	1.8261
Tip clearance $Y$ ( $\delta = 1.82 \times 10^{-3}$ m)	10	0.001	0.999	0.02764	0.0087	Normal	

**Table 4** BTRRC reliability analytical results

Type	$Y_d$	$Y_b$	$Y_c$
Sen	0.763	0.72	–0.483
Pa	0.388	0.366	0.246

**Table 5** Sensitivity analysis results of  $Y_d$ ,  $Y_b$  and  $Y_c$ 

Methods	Fitting response surface models			Simulation time of different simulation number (s)				
	Fitting time (s)	Sample number	Time of one calculation (s)	$10^2$	$10^3$	$10^4$	$10^5$	$10^6$
MC method	–			$1.165 \times 10^5$	$9.897 \times 10^5$	–	–	–
T-LSSVM	$3.791 \times 10^5$	381	32.875	0.872	5.491	49.872	487.192	4793.563
DCRSM	$1.711 \times 10^3$	49	34.918	0.143	1.009	11.517	117.786	1385.485
DC-T-LSSVM	$1.364 \times 10^4$	30	11.367	0.093	0.629	7.293	57.669	459.571

**Table 6** Computing time for the BTRRC probabilistic analysis